

# Convergent NMPC-based Reinforcement Learning Using Deep Expected Sarsa and Nonlinear Temporal Difference Learning

Amine Salaje, Thomas Chevet, and Nicolas Langlois

**Abstract**—In this paper, we present a learning-based nonlinear model predictive controller (NMPC) using an original reinforcement learning (RL) method to learn the optimal weights of the NMPC scheme. The controller is used as the current action-value function of a deep Expected Sarsa where the subsequent action-value function, usually obtained with a secondary NMPC, is approximated with a neural network (NN). With respect to existing methods, we add to the NN's input the current value of the NMPC's learned parameters so that the network is able to approximate the action-value function and stabilize the learning performance. Additionally, with the use of the NN, the real-time computational burden is approximately halved without affecting the closed-loop performance. Furthermore, we combine gradient temporal difference methods with parametrized NMPC as function approximator of the Expected Sarsa RL method to overcome the potential parameters divergence and instability issues when nonlinearities are present in the function approximation. The simulation result shows that the proposed approach converges to a locally optimal solution without instability problems.

## I. INTRODUCTION

Nonlinear model predictive control (NMPC) has proven effective in addressing complex control challenges [1], particularly in systems with nonlinear dynamics and constraints, such as mobile robotics [2]. It generates control signals by solving a constrained optimization problem – the optimal control problem (OCP) – at each time step. However, fine-tuning the parameters of the OCP remains a challenge, with ongoing research seeking reliable tuning methods [3]. Reinforcement learning (RL) offers a promising solution as it enables an agent to optimize these parameters by learning optimal value functions and policies within the scope of a Markov decision process (MDP) [4].

In problems with large MDPs or high-dimensional state spaces, modern RL methods often use deep neural networks (DNN) to approximate value functions or policies, allowing them to handle the complexity of nonlinear systems. However, DNN-based RL approaches often face difficulties in closed-loop stability analysis and can be challenging for formal verification and constraint management [5], thus raising concerns about ensuring safety in control systems. To address these issues, NMPC-based RL has been proposed and justified in [5] as a promising solution. By using the OCP as a function

approximator for the optimal policy in RL, this approach naturally satisfies state and input constraints while ensuring safety requirements.

In [5], the NMPC parameters are tuned to enhance closed-loop performance using Q-learning and policy gradient RL methods. Since then, various studies have deployed Q-learning with MPC as a function approximator to realize this task, with notable contributions found in [6]–[10]. However, one of the current challenges of these approaches is the significant computational demand for real-time implementation [11]. Indeed, in the context of temporal difference (TD) learning methods, it is required to solve at least two constrained nonlinear optimization problems at each sampling instant – one for estimating the current action-value function and another for approximating the subsequent action-value function.

To deal with this issue, a new data-driven approach was proposed in [12], where a parametrized NMPC has been used as an approximator for a deep double Expected Sarsa (ES) RL method. To estimate the current action-value function, a parametrized OCP is solved at each time step. However, the subsequent action-value function is approximated using a target neural network (NN) instead of solving a second OCP at the next time step. The NN is trained with inputs and outputs of the primary NMPC obtained at previous sampling times. This approach shows a clear advantage in reducing online computation time compared to [5]. However, as the second NMPC of [5] is replaced by a NN in [12], the simulation results show lack of stability and potential divergence. As a first contribution, we propose in the present paper to tackle this problem by adding the parametrization vector of the NMPC at previous time steps to the training input of the NN, leading to a clear improvement in the convergence stability and control performance compared with [12].

While simple to use, conventional TD learning methods such as Q-learning do not come with formal guarantees regarding the closed-loop optimality of the resulting policy [4]. Furthermore, they lack convergence guarantees when using non linear function approximation, which may cause potential divergence of the approximator parameters. To overcome these challenges, the authors of [13] proposed gradient temporal difference (GTD) for off-policy Q-learning methods as an effective solution, and proven to almost-sure convergence for any finite MDP and any smooth value function approximator to a locally optimal solution or equilibrium point. As a second contribution, we combine in this paper GTD methods with parametrized NMPC as function approximator in the Expected Sarsa (ES) RL method to overcome the potential parameters divergence and instability issues. To the best of the authors'

\*This work was supported by ANR and Région Normandie through the HAISCoDe (ANR-20-THIA-0021) and PAMAP projects.

For this reason and the purpose of Open Access, the authors have applied a CC BY public copyright licence to any Author Accepted Manuscript (AAM) version arising from this submission.

The authors are with Université de Rouen, ESIGELEC, IRSEEM, 76000 Rouen, France amine.salaje@groupe-esigelec.org, {thomas.chevet, nicolas.langlois}@esigelec.fr

knowledge, this is the first work where an action-value method is used to tune the NMPC approximator using GTD methods. The simulation results shows that the proposed approach converges to a locally optimal solution without instability problems compared to previous methods.

The remainder of this article is organized as follows. Section II exposes prerequisites on predictive control and reinforcement learning. Then, Section III presents our contributions. Finally, Section IV showcases the efficiency of our methods on numerical simulation examples.

## II. PREREQUISITES ON LEARNING AND CONTROL

We start by giving some context on the considered control strategy and background on the RL methods we use.

### A. Markov decision process for RL

Consider the tuple  $(\mathcal{S}, \mathcal{A}, \mathbb{P}, \ell, \rho, \gamma)$  which defines an MDP with continuous state space  $\mathcal{S} \subseteq \mathbb{R}^n$  and action space  $\mathcal{A} \subseteq \mathbb{R}^m$ . The state transition dynamics have the underlying probability law  $\mathbb{P}$  such that  $\mathbf{s}_{k+1} \sim \mathbb{P}(\cdot | \mathbf{a}_k, \mathbf{s}_k)$ , with  $\mathbf{s}_{k+1}, \mathbf{s}_k \in \mathcal{S}$  and  $\mathbf{a}_k \in \mathcal{A}$ . In a control approach, these state transition dynamics can be expressed as  $\mathbf{s}_{k+1} = f(\mathbf{a}_k, \mathbf{s}_k)$  where  $f$  is the discretized real system dynamics. The remaining elements of the tuple are the reward  $\ell$ , or stage cost in optimal control, associated to each MDP transition, the initial state distribution  $\rho$ , and the discount factor  $\gamma \in (0, 1)$  determining the importance of future rewards.

The goal of RL is to find a policy, denoted by  $\pi: \mathcal{S} \rightarrow \mathcal{A}$ , minimizing a closed-loop performance objective [4]. Consider then a deterministic policy delivering the control input  $\mathbf{a}_k = \pi(\mathbf{s}_k)$  resulting in state distribution  $\rho^\pi$ . Given an objective  $J(\pi) = \mathbb{E}_{\mathbf{s} \sim \rho^\pi} \left[ \sum_{k=0}^K \gamma^k \ell(\mathbf{s}_k, \mathbf{a}_k) \middle| \mathbf{a}_k = \pi(\mathbf{s}_k) \right]$  on the expected discounted cumulative cost, with  $K \in \mathbb{N} \cup \{+\infty\}$  a (possibly infinite) horizon, the RL problem aims to find the optimal policy  $\pi^*$  satisfying  $\pi^* = \arg \min J(\pi)$ .

The optimal action-value function  $Q^*(\mathbf{s}_k, \mathbf{a}_k)$  and value function  $V^*(\mathbf{s}_k)$  associated to the optimal policy  $\pi^*$  can be determined by using the Bellman equations

$$\begin{aligned} Q^*(\mathbf{s}_k, \mathbf{a}_k) &= \ell(\mathbf{s}_k, \mathbf{a}_k) + \gamma \mathbb{E}[V^*(\mathbf{s}_{k+1}) | \mathbf{s}_k, \mathbf{a}_k], \\ V^*(\mathbf{s}_k) &= Q^*(\mathbf{s}_k, \pi^*(\mathbf{s}_k)) = \min Q^*(\mathbf{s}_k, \mathbf{a}_k). \end{aligned} \quad (1)$$

### B. NMPC as a function approximator

As in [5], we use a parametric optimization problem as a function approximator for the reinforcement learning. We therefore consider the parametrized NMPC

$$\begin{aligned} \min_{\substack{\mathbf{u}_i, \mathbf{x}_i, \sigma_i, \\ \forall i \in \overline{0, N}}} & \sum_{i=0}^{N-1} \gamma^i (L(\mathbf{x}_i, \mathbf{u}_i, \boldsymbol{\vartheta}) + \boldsymbol{\omega}^\top \boldsymbol{\sigma}_i) \\ & + \gamma^N (V(\mathbf{x}_N, \boldsymbol{\vartheta}_f) + \boldsymbol{\omega}_f^\top \boldsymbol{\sigma}_N) \quad (2a) \\ \text{s.t.} & \quad \mathbf{x}_0 = \mathbf{s}_k, \quad (2b) \\ & \quad \mathbf{x}_{i+1} = f(\mathbf{u}_i, \mathbf{x}_i), \quad \forall i \in \overline{1, N}, \quad (2c) \\ & \quad \mathbf{x}_i \in \mathcal{S}, \quad \forall i \in \overline{1, N}, \quad (2d) \\ & \quad \mathbf{u}_i \in \mathcal{A}, \quad \forall i \in \overline{0, N-1}, \quad (2e) \\ & \quad g(\mathbf{x}_i) + \theta_c \leq \boldsymbol{\sigma}_i, \boldsymbol{\sigma}_i \geq 0, \quad \forall i \in \overline{0, N}, \quad (2f) \end{aligned}$$

In this formulation,  $\forall i \in \overline{0, N}$ , the variables  $\mathbf{u}_i$ ,  $\mathbf{x}_i$ , and  $\boldsymbol{\sigma}_i$  represent the primal decision variables,  $L$  the NMPC stage cost and  $V$  the terminal cost. The prediction horizon  $N \in \mathbb{N}$  may be shorter than  $K$  from the performance measure  $J(\pi)$ , and  $\gamma$  is the discount factor referenced in Paragraph II-A. The function  $f$  denotes the deterministic dynamic model driven by the NMPC scheme (2) as in Paragraph II-A, while the function  $g$  imposes additional constraints on the state at each time step over the prediction horizon  $N$ . The variables  $\boldsymbol{\sigma}_i$ , for  $i \in \overline{0, N}$ , are slack variables introduced to relax state constraints, with their violation penalized by the weights  $\boldsymbol{\omega}$  and  $\boldsymbol{\omega}_f$ , preventing the potential infeasibility of the NMPC due to the additional constraints. Finally,  $\boldsymbol{\vartheta}$  and  $\boldsymbol{\vartheta}_f$  are vectors of NMPC weights, usually selected *a priori* based, e.g., on the dynamics  $f$  or the control objective for the system. In this paper, these weights are treated as parameter vectors to be adjusted through an RL algorithm.

Indeed, an RL algorithm can advantageously adjust the parameters of the NMPC cost function, model, and constraints in a way to enhance closed-loop performance. In theory, as stated in [5, Theorem 1], under specific assumptions and with a sufficiently expressive parametrization, the MPC scheme can approximate the optimal policy  $\pi^*$ .

When solving (2) at time  $k \in \mathbb{N}$ , we obtain the optimal control sequence  $\mathbf{u}^*(\mathbf{s}_k, \boldsymbol{\theta}) = \{\mathbf{u}_0^*(\mathbf{s}_k, \boldsymbol{\theta}), \dots, \mathbf{u}_{N-1}^*(\mathbf{s}_k, \boldsymbol{\theta})\}$ , with  $\boldsymbol{\theta} = [\boldsymbol{\vartheta} \quad \boldsymbol{\vartheta}_f]$  driving the system with dynamics (2c) towards its objective over the prediction horizon  $N$ .

### C. Expected Sarsa with NMPC as function approximator

ES is a TD control method used in model-free reinforcement learning [4]. To handle large MDPs, the ES algorithm employs function approximators parametrized by unknown parameters  $\boldsymbol{\theta}$  to approximate the optimal action-value function  $Q^*$ .

Under some assumptions given in [5], the NMPC scheme (2) approximates the optimal action-value function  $Q^*$ . Thus, for any  $k \in \mathbb{N}$ , we define

$$Q_\theta(\mathbf{s}_k, \mathbf{a}_k) = (2), \quad (3)$$

an approximator of the optimal action-value function  $Q^*$ . The policy  $\pi_\theta(\mathbf{s}_k)$  and the action  $\mathbf{a}_k$  are obtained by solving (2), so that, for any  $\mathbf{s}_k \in \mathcal{S}$ ,

$$\pi_\theta(\mathbf{s}_k) = \arg \min_{\mathbf{a}_k \in \mathcal{A}} Q_\theta(\mathbf{s}_k, \mathbf{a}_k) = \mathbf{u}_0^*(\mathbf{s}_k, \boldsymbol{\theta}), \quad (4)$$

$$\mathbf{a}_k = \pi_\theta(\mathbf{s}_k) + c_\varepsilon^k \boldsymbol{\varepsilon} \quad (5)$$

satisfying the Bellman equation [4]. Here,  $\boldsymbol{\varepsilon} \sim \mathcal{N}(0, 1)$  represents a Gaussian term that introduces weighted exploration of the continuous action space  $\mathcal{A}$ . This exploration decreases exponentially during training due to the factor  $c_\varepsilon \in (0, 1)$ . During the learning process, the action  $\mathbf{a}_k$  defined by (5), is applied to the system at time step  $k$ , resulting in  $\mathbf{s}_{k+1}$ .

To simplify the notations, the time dependence is dropped for states  $\mathbf{s} \in \mathcal{S}$  and actions  $\mathbf{a} \in \mathcal{A}$ . Then,  $\mathbf{s}^+ \in \mathcal{S}$  denotes the state at the next time instant.

In order to find  $Q^*$ , we characterize the optimal parameters  $\theta^*$  as those minimizing the least-squares problem

$$\theta^* = \arg \min_{\theta} \mathbb{E}_{\pi_{\theta}} \left[ \frac{1}{2} (Q^*(s, \mathbf{a}) - Q_{\theta}(s, \mathbf{a}))^2 \right]. \quad (6)$$

Since the optimal  $Q^*$  is unknown, we cannot solve (6) directly. To do so, we use here the continuous ES algorithm [14].

The parametrized action-value function  $Q_{\theta}$  is estimated using the NMPC scheme (2) parametrized by the vector  $\theta$ . At each sampling time, the parameters are updated based on the TD error

$$\delta = \ell(s, \mathbf{a}) + \gamma Q_{\theta}(s^+, \mathbf{a}^+) - Q_{\theta}(s, \mathbf{a}) \quad (7)$$

where  $\mathbf{a}^+$  is obtained by applying  $\mathbf{a}$ , obtained as in (5) by solving the OCP (2) for state  $s$  (behavioral policy), to the controlled system and solving again the OCP (2) for the resulting state  $s^+$  (target policy). The parameter updates are determined by minimizing the mean-square TD error (MSTDE)

$$\min_{\theta} \mathbb{E}_{\pi_{\theta}} \left[ \frac{1}{2} (\ell(s, \mathbf{a}) + \gamma Q_{\theta}(s^+, \mathbf{a}^+) - Q_{\theta}(s, \mathbf{a}))^2 \right]. \quad (8)$$

We apply the semi gradient step to perform this minimization, thus giving the parameters update rule

$$\theta \leftarrow \theta + \alpha \delta \nabla_{\theta} Q_{\theta}(s, \mathbf{a}) \quad (9)$$

where  $\alpha > 0$  is the learning rate. By updating the unknown parameters, the action-value functions can converge towards its optimal value. The gradient  $\nabla_{\theta} Q_{\theta}(s, \mathbf{a})$  is presented in Paragraph III-B.

The choice of using NMPC as function approximator of the ES rather than Q-learning provides several advantages, in terms of control performance, exploration capabilities and straight-forward implementation [10].

### III. PROPOSED METHODS

This section presents the main contributions of this paper, aiming to improve the overall performances of the learning algorithm. Our methods are then summarized in Algorithm 1.

#### A. Reducing computational complexity of NMPC-based ES

1) **Problem definition:** In [5] and [10], the parameter vector  $\theta$  is tuned using a Q-learning and an ES algorithm, respectively. In both cases, it is required to solve, at each learning step, a first OCP of the form (2) to obtain  $Q_{\theta}(s, \mathbf{a})$  as well as a second OCP to obtain the subsequent action-value function  $Q_{\theta}(s^+, \mathbf{a}^+)$ . These two action-value functions are then used to compute the TD error to be minimized. However, solving two constrained nonlinear optimization problems at each time step significantly increases the real-time computational complexity, resulting in longer training times. This issue worsens with large prediction horizons  $N$ , when the OCP (2) involves multiple constraints, etc. To address this problem, [12] replace the second OCP of the aforementioned methods by a neural network approximator. However, this method may diverge due to an inaccurate approximation of the subsequent action-value function.

2) **NMPC-based regularized deep ES (RDES):** To better approximate the subsequent action-value function obtained with a second NMPC [10] using a NN, we propose to adjust the input data used to train the NN. The idea is to learn the action-value function  $Q_{\theta}$  of (3) using a neural network  $Q_{\varpi_{\text{NN}}}$  parametrized by the weights  $\varpi_{\text{NN}}$  so that  $Q_{\varpi_{\text{NN}}}(s, \mathbf{a}, \theta) \approx Q_{\theta}(s, \mathbf{a})$ . To do so, the NN training input should be chosen carefully.

In order to train the NN, we store, at each learning step, the tuple  $\{s, \mathbf{a}, \theta, Q_{\theta}(s, \mathbf{a})\}$  into a replay buffer  $\mathcal{D}$ . The current state  $s$ , the action  $\mathbf{a}$  and the parametrization vector  $\theta$  are the NN's inputs while  $Q_{\theta}(s, \mathbf{a})$  is the regression target. Then, a mini-batch  $\mathcal{B} \subset \mathcal{D}$  of  $n \in \mathbb{N}$  elements is randomly sampled and we update  $\varpi_{\text{NN}}$  using the Adam algorithm [15] with a learning rate  $\zeta$  to minimize the cost function

$$C_{\text{NN}}(\theta) = \frac{1}{n} \sum_{\{\zeta, \eta, \vartheta, q\} \in \mathcal{B}} (Q_{\varpi_{\text{NN}}}(\zeta, \eta, \vartheta) - q)^2 \quad (10)$$

where  $Q_{\varpi_{\text{NN}}}(\zeta, \eta, \vartheta)$  for  $\{\zeta, \eta, \vartheta, q\} \in \mathcal{B} \subset \mathcal{D}$  is the output of the NN with parameters  $\varpi_{\text{NN}}$  and inputs  $\zeta$ ,  $\eta$ , and  $\vartheta$ , whereas  $q$  is the regression target.

After the NN's update, the subsequent action-value function in (7) is predicted by passing to the NN the next state  $s^+$  and the new target policy defined as  $\mathbf{a}^+ = \pi_{\theta}(s^+) = \mathbf{u}_1^*(s, \theta)$  the optimal value of  $\mathbf{u}_1$ , the second input vector over the prediction horizon when solving the primary NMPC (4). By doing so, only one constrained optimization problem needs to be solved at each time step as well as the NN optimization process. Finally, we define the new TD error to be minimized, at each learning step, by

$$\varrho = \ell(s, \mathbf{a}) + \gamma Q_{\varpi_{\text{NN}}}(s^+, \mathbf{a}^+, \theta) - Q_{\theta}(s, \mathbf{a}). \quad (11)$$

Compared with [10], our contribution then consists in adjusting the input data used to train the NN. We incorporate the current value of the parametrization vector  $\theta$  of the action-value function defined in (3) to the NN's input. This is based on the assumption that the approximated subsequent action-value function should depend on  $\theta$ , as the current action-value function takes vector  $\theta$  as input at each time step. Thus, by adding the parameter vector  $\theta$  to the training data, the NN gains more knowledge about the behavior of the primary NMPC (2). Therefore, stabilizing the learning performance and improving the approximation of the action-value function, which is usually computed by solving a second NMPC, we have

$$Q_{\varpi_{\text{NN}}}(s, \mathbf{a}, \theta) \rightarrow Q_{\theta}(s, \mathbf{a}). \quad (12)$$

#### B. Nonlinear temporal difference learning

1) **Problem definition:** Traditional TD methods like Q-learning and ES have been successfully applied with function approximation in various fields. However, it is well-known that these algorithms can become unstable, particularly when off-policy sampling or nonlinear function approximation is used, which can lead to parameter divergence in the approximator. To address this issue, we build on the results from [13], [16], and our idea is to use a GTD approach to solve the instability and convergence issues when using

NMPC as function approximator of RL methods. Indeed, the GTD methods are proven to converge almost surely, for any MDP and even with nonlinear function approximators, to a locally optimal solution or equilibrium point.

2) **Convergent NMPC-based gradient ES (GES):** In TD learning control methods, most works use an objective function representing how closely the approximate action-value function satisfies the Bellman equations. The true action-value function satisfies the Bellman equation in model-free RL

$$\Gamma^\pi Q(\mathbf{s}, \mathbf{a}) = \mathbb{E}_\pi [\ell(\mathbf{s}, \mathbf{a}) + \gamma Q(\mathbf{s}^+, \mathbf{a}^+)] \quad (13)$$

where  $\Gamma^\pi$  is known as the Bellman operator. In GTD approaches, the objective function that measure how closely the approximation  $Q_\theta(\mathbf{s}, \mathbf{a})$  satisfies the Bellman equation (13) is known as the mean-square projected Bellman error (MSPBE), where the goal is to minimize

$$\mathfrak{J}(\theta) = \|\Pi(\Gamma^{\pi_\theta} Q_\theta) - Q_\theta\|_{\rho^\pi}^2 \quad (14)$$

using approximate gradient decent,  $\Pi$  is a projection operator which projects action-value functions into the linear space  $\mathcal{F} = \{Q_\theta : \theta \in \mathbb{R}^d\}$  w.r.t  $\|\cdot\|_{\rho^\pi} : \Pi(\hat{Q}) = \arg \min_{f \in \mathcal{F}} \|\hat{Q} - f\|_{\rho^\pi}$ .

Following [13], the projected objective can be written in terms of expectations as

$$\mathfrak{J}(\theta) = \mathbb{E}[\delta\phi]^\top \mathbb{E}[\phi\phi^\top]^{-1} \mathbb{E}[\delta\phi], \quad (15)$$

where  $\delta$  is the TD error as in (7), and  $\phi$  is the feature vector used in approximating the action-value function. In [13], the authors used an unrestricted linear form for the action-value function approximation, specifically  $Q_\theta(\mathbf{s}, \mathbf{a}) = \phi^\top \theta$ . However, in this paper, we use a nonlinear function approximation defined by the OCP scheme (2), making it challenging to directly obtain the associated feature vector. Therefore, we represent  $\phi$  as the gradient of the action-value function, expressed as  $\phi = \nabla_\theta Q_\theta(\mathbf{s}, \mathbf{a})$ .

Finally, by applying the negative gradient on the MSPBE objective function, and introducing a new set of weights  $\mathbf{w}$  making use of the weight doubling trick (the interested reader can refer to [13], [16], [17] for details), we get the update rules

$$\begin{aligned} \theta &\leftarrow \theta + \alpha [\delta\phi - \gamma (\mathbf{w}^\top \phi) \phi^+], \\ \mathbf{w} &\leftarrow \mathbf{w} + \beta [\delta - \phi^\top \mathbf{w}] \phi, \end{aligned} \quad (16)$$

where  $\phi^+$  is the subsequent action-value features  $\nabla_\theta Q_\theta(\mathbf{s}^+, \mathbf{a}^+)$ . Under some assumptions [13] on the positive step sizes  $\alpha, \beta > 0$ , it follows that  $\theta$  converges almost surely to a stable equilibrium point.

3) **Sensitivity analysis:** This paragraph explains the process for computing  $\nabla_\theta Q_\theta(\mathbf{s}, \mathbf{a})$ , the gradient appearing in the GES update rule (16). This approach is inspired by the work of [5]. Let  $\mathcal{L}_\theta$ , the Lagrangian function associated to the NMPC scheme (2), be

$$\mathcal{L}_\theta(\mathbf{z}) = \Omega_\theta + \boldsymbol{\mu}^\top \mathbf{H}_\theta, \quad (17)$$

where  $\Omega_\theta$  represents the parametrized NMPC cost function (2a) and  $\mathbf{H}_\theta$  is a vector stacking vertically the inequality

---

**Algorithm 1:** Learning algorithm.

---

```

1 Input:  $\theta, \mathbf{w}, \varpi_{\text{NN}}$ , dynamical system  $f$ , NMPC (2)
2 Output:  $\theta^*$ 
3 Initialization:  $\mathcal{D} \leftarrow \emptyset$ 
4 for  $k \leftarrow 1$  to  $N_{\text{episode}}$  do
5    $\mathbf{s} \leftarrow \mathbf{s}_0$ 
6   for  $t \leftarrow 0$  to  $K$  do
7     Solve (2) in  $\mathbf{s}$  to obtain  $\mathbf{a}$ , and  $Q_\theta(\mathbf{s}, \mathbf{a})$ 
8     Get the action  $\mathbf{a}$  from (5)
9     Observe  $\mathbf{s}^+ = f(\mathbf{a}, \mathbf{s})$  and get the reward  $\ell$ 
10    if RDES used then
11      Store  $\mathcal{D} \leftarrow \mathcal{D} \cup \{\mathbf{s}, \mathbf{a}, \theta, Q_\theta(\mathbf{s}, \mathbf{a})\}$ 
12      if  $\text{Card}(\mathcal{D}) \geq n$  then
13        Randomly sample mini-batch of  $n$ 
14        elements of  $\mathcal{D}$  and get  $\varpi_{\text{NN}}$  from
15        (10)
16        Compute the TD error  $\delta$  with (11)
17        Update parameters  $\theta$  by (9)
18      else if GES used then
19        Solve (2) in  $\mathbf{s}^+$  to obtain  $Q_\theta(\mathbf{s}^+, \mathbf{a}^+)$ 
20        Compute the TD error  $\delta$  with (7)
21        Update parameters  $\theta$  and  $\mathbf{w}$  by (16)
22     $\mathbf{s} \leftarrow \mathbf{s}^+$ 

```

---

constraints appearing in problem (2). The real vector  $\boldsymbol{\mu}$  denotes the Lagrange multiplier associated to the inequality constraint, having the size of  $\mathbf{H}_\theta$ . Let  $\mathbf{z} = \{\mathbf{x}, \mathbf{u}, \boldsymbol{\sigma}, \boldsymbol{\mu}\}$  be the primal-dual variables solution of the NMPC obtained from solving (2). Consequently, the sensitivity of the action-value function with respect to the parametrization  $\theta$  is written as

$$\nabla_\theta Q_\theta(\mathbf{s}, \mathbf{a}) = \nabla_\theta \mathcal{L}_\theta(\mathbf{z}). \quad (18)$$

#### IV. NUMERICAL APPLICATIONS

In this section we apply both our RL-based methods to the case of setpoint tracking problem with static obstacle avoidance for a diff-drive mobile robot. These simulations aim to show the clear improvement in the methods we propose compared with the methods from [10] and [12].

##### A. Simulation model

We consider a diff-drive robot having for continuous-time dynamics [18]

$$\dot{x} = v \cos \varphi, \quad (19a)$$

$$\dot{y} = v \sin \varphi, \quad (19b)$$

$$\dot{\varphi} = \nu. \quad (19c)$$

The robot's state is defined by its coordinates  $(x, y)$  in a two-dimensional plane, linear speed  $v$ , and orientation  $\varphi$ . For training, we discretize the dynamics (19) using the Runge-Kutta 4 method with a sampling period of  $T_s = 0.2$  s, so that

$$\mathbf{s}_{k+1} = f(\mathbf{u}_k, \mathbf{s}_k), \quad (20)$$

where  $\mathbf{s}_k^\top = [x_k \ y_k \ \varphi_k]$  and  $\mathbf{u}_k^\top = [v_k \ \nu_k]$ .

The robot objective is to find the shortest path to reach an equilibrium point ( $\mathbf{s}^{\text{ref}}, \mathbf{u}^{\text{ref}}$ ) of the dynamics (20), starting from a given initial position  $\mathbf{s}_0$ . Here  $\mathbf{s}^{\text{ref}}$  denotes the desired target state vector. Along its trajectory, the robot must maintain a desired safe distance from obstacles. To accomplish this objective, the robot is controlled using an NMPC as defined in (2). The cost function (2a) is designed such that, for any  $i \in 0, N-1$ ,

$$L(\mathbf{s}_i, \mathbf{u}_i, \boldsymbol{\theta}) = \|\mathbf{s}_i - \mathbf{s}^{\text{ref}}\|_{\text{diag}(\boldsymbol{\vartheta}_x)}^2 + \|\mathbf{u}_i - \mathbf{u}^{\text{ref}}\|_{\text{diag}(\boldsymbol{\vartheta}_u)}^2, \\ \Gamma(\mathbf{s}_N, \boldsymbol{\theta}) = \|\mathbf{s}_N - \mathbf{s}^{\text{ref}}\|_{\text{diag}(\boldsymbol{\vartheta}_f)}^2$$

where  $\text{diag}(\boldsymbol{\theta})$  is a diagonal matrix having for elements the components of  $\boldsymbol{\theta}$ , with  $\boldsymbol{\vartheta}_x = [\theta_x \ \theta_y \ \theta_\varphi]$ ,  $\boldsymbol{\vartheta}_u = [\theta_v \ \theta_\nu]$ , and  $\boldsymbol{\vartheta}_f = [\theta_{x_f} \ \theta_{y_f} \ \theta_{\varphi_f}]$ , and  $\|\mathbf{x}\|_Q^2 = \mathbf{x}^\top Q \mathbf{x}$ .

The action space is  $\mathcal{A} = [-0.6 \text{ m} \cdot \text{s}^{-1}, 0.6 \text{ m} \cdot \text{s}^{-1}] \times [-\pi/2, \pi/2]$ . The state space is  $\mathcal{S} = [-9 \text{ m}, 3 \text{ m}] \times [-9 \text{ m}, 3 \text{ m}] \times \mathbb{R}$ . The robot has to stay at a given distance from 4 obstacles by satisfying the inequality constraint (2f), defined, for  $n \in \overline{1, 4}$ , as

$$1 - 4 \underbrace{\frac{(x_i - x_{\text{obs},n})^2 + (y_i - y_{\text{obs},n})^2}{(d_{\text{rob}} + d_{\text{obs}})^2}}_{\Xi(\mathbf{x}_i)} + \theta_c \leq 0, \quad (21)$$

where  $(x_{\text{obs},n}, y_{\text{obs},n})$  is the center of the  $n$ -th obstacle, while  $d_{\text{rob}} = 0.5 \text{ m}$  and  $d_{\text{obs}} = 2 \text{ m}$  represents the diameters of a safety circle surrounding the robot and an obstacle, respectively. Parameter  $\theta_c$  serves as a tuning variable, adjusting the intensity of the collision avoidance constraints. Overall, the parameters vector is  $\boldsymbol{\theta} = [\theta_x \ \theta_y \ \theta_\varphi \ \theta_v \ \theta_\nu \ \theta_{x_f} \ \theta_{y_f} \ \theta_{\varphi_f} \ \theta_c]^\top$ .

To train the RL agent, the robot's initial state is set as  $\mathbf{s}_0^\top = [-2.5 \text{ m} \ 1.5 \text{ m} \ 0 \text{ rad}]$ , and the target state is defined as  $\mathbf{s}^{\text{ref}} = [8.5 \text{ m} \ 2 \text{ m} \ \pi/2]^\top$ , with the reference input  $\mathbf{u}^{\text{ref}} = \mathbf{0}$ . The vectors  $\mathbf{s}_0$  and  $\mathbf{s}^{\text{ref}}$  remain fixed throughout all learning episodes. The RL stage cost  $\ell$  used to evaluate the RL performance defined in Paragraph II is

$$\ell = \begin{cases} \|\mathbf{s}_k - \mathbf{s}^{\text{ref}}\|_Q^2 + \|\mathbf{u}_k\|_2 & \text{if } \|\mathbf{s}_k - \mathbf{s}^{\text{ref}}\|_2 < d_t \\ \|\mathbf{s}_k - \mathbf{s}^{\text{ref}}\|_Q^2 + \Upsilon(\mathbf{s}_k) & \text{if } \|\mathbf{s}_k - \mathbf{s}^{\text{ref}}\|_2 \geq d_t \end{cases}, \quad (22)$$

where  $Q = \text{diag}(1, 1, 0.1)$  is the objective weighting matrix,  $d_t = 1.5 \text{ m}$  is a constant distance threshold, and  $\Upsilon(\mathbf{s}_k) = \sum_{n=1}^4 c \max\{0, \Xi(\mathbf{s}_k) + d_o\}$  is the obstacle penalty collision where  $\Xi$  is as defined as in (21), and  $d_o = 0.35 \text{ m}$  is a desired safe distance between the robot and the obstacle, and  $c = 50$  is a penalty weight. If a collision occurs,  $\Upsilon(\mathbf{s}_k)$  adds a positive penalty to the RL stage cost  $\ell$ .

### B. Simulation results

To showcase the advantages of our algorithm, we train  $\boldsymbol{\theta}$  for 300 episodes in four ways: one using the method from [10], one using the method from [12], and the last two using the proposed methods from paragraphs III-A and III-B. The numerical computation is performed using the Ipopt solver provided by the CasADi software framework [19] on a PC equipped of 16 GB of RAM.

TABLE I  
CONTROLLER AND ALGORITHM CONFIGURATION.

Parameter	Value
$\alpha, \beta, \zeta$	$10^{-7}, 10^{-8}, 10^{-2}$
$\mathbf{w}_{\text{init}}$	$10^{-4}$
Robot $\boldsymbol{\theta}_{\text{init}}$	$[1 \ 1 \ 0.05 \ 0.05 \ 0.05 \ 1 \ 1 \ 0.1 \ 0.001]$
Law of $\boldsymbol{\rho}, \gamma$	$\mathcal{N}(0, 1), 0.97$
$N, K, N_{\text{ep}}$	10, 129, 300
$\boldsymbol{\omega}, \boldsymbol{\omega}_f$	$[100, 100, 100, 100]^\top$
Mini-batch size $\text{card}(\mathcal{B})$	128
Hidden layers, neurons per layer	2, 64

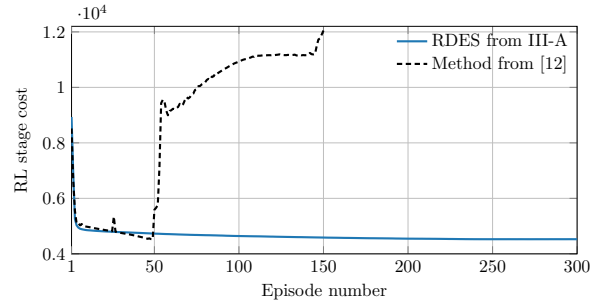


Fig. 1. RL stage cost  $\ell$  sum over learning episodes.

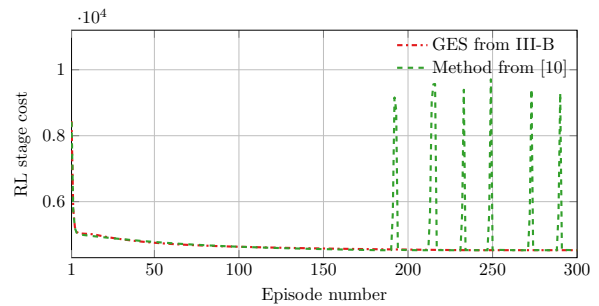


Fig. 2. RL stage cost  $\ell$  sum over learning episodes.

For fair comparison, we compare the deep ES method from [12] with our RDES method from paragraph III-A. Indeed, for both these methods, only one NMPC must be solved to compute the current action-value function, whereas the subsequent action-value function is approximated by a neural network. Fig. 1 shows the sum of RL stage cost across training episodes for both approaches. In the red graph, we can observe that the RL performance decreases faster, with the learning process remaining stable throughout training episodes, highlighting the effect of adding the parametrization vector into the NN's training input for better approximation of the subsequent action-value function. In contrast, the blue graph from [12] shows divergent RL performance, likely due to inaccuracies in approximating the subsequent action-value function.

To demonstrate the effectiveness of our second contribution from Paragraph III-B, we compare our proposed GES with the ES method from [10]. In both approaches, two NMPCs are solved to compute the TD error in (7). As we already stated, conventional temporal-difference learning methods can become unstable or even diverge when nonlinear function

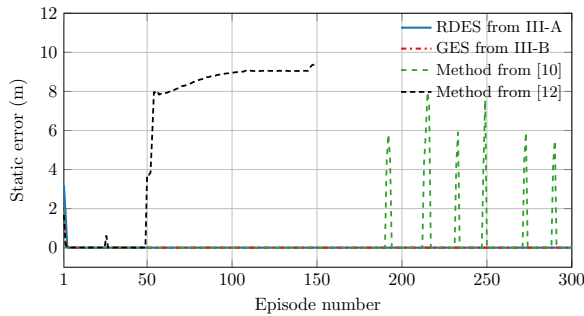


Fig. 3. Static errors over the training episodes.

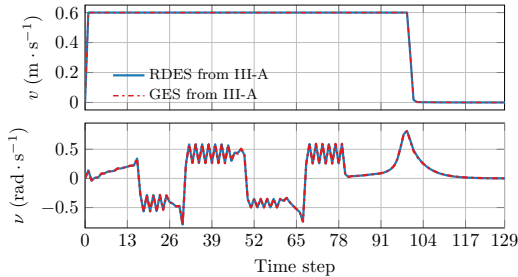


Fig. 4. Robot control signals under the learned policies.

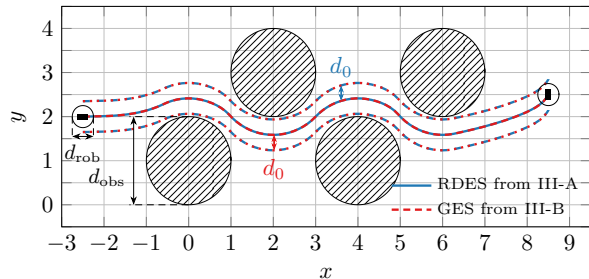


Fig. 5. Robot states' trajectories under the learned policies.

approximation is involved. In Fig.2, we see that the blue graph reflects an unstable learning process as training episodes progress, attributed to the nonlinearities in the NMPC function approximator. In contrast, the red graph displays stable RL performance, with the GES method converging toward a stable equilibrium point. This demonstrates the effectiveness of GTD learning, which is a true gradient descent method, ensures convergence.

In Fig. 3, we present the static error, i.e., the distance of the robot's state at the end of an episode  $s_{129}$  to the objective  $s^{ref}$ . This figure illustrates the learning stability achieved by our proposed methods, opposed to the instability observed in [10] and the divergence noted in [12].

Figs. 4 and 5 present a comparison of the control signals and the robot's trajectories for both proposed methods. First, we observe that the input actions satisfy their constraints across both approaches. Additionally, we see that in both cases, the robot successfully reaches the target state, maintaining a safe distance  $d_0$  from each obstacle, as required by the RL stage cost (22), which shows the optimal policy achieved

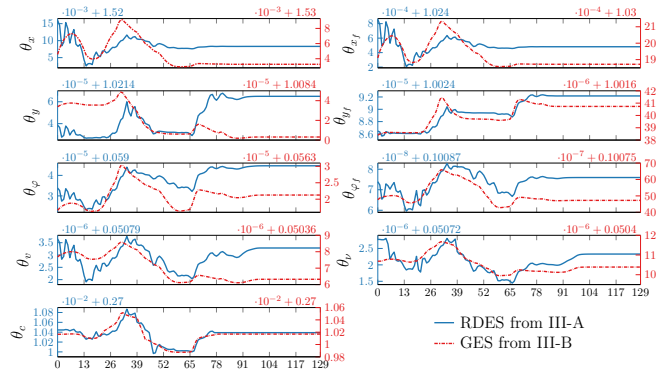


Fig. 6. Tuned parameters under the learned policy of the proposed GES.

TABLE II  
TRAINING TIME COMPARISON.

Method	Training time (h)
NMPC-based ES from [10]	$\approx 18$
NMPC-based GES from III-B	$\approx 18$
NMPC-based RDES from III-A	$\approx 9$

by our methods. Finally, Fig. 6 illustrates the variation of the tuned parameters  $\theta$  over the last training episode using the RDES and GES from Paragraphs III-A and III-B, respectively.

Table II presents the real-time training duration of the three methods for 300 learning episodes. The deep ES method from [12] is excluded, as it diverges before reaching the 300th episode. As shown, our RDES method completes the training episodes in half the time required for both the method from [10] and our GES method.

## V. CONCLUSION

In this paper we propose two original reinforcement learning-based methods for tuning the parameters of a nonlinear model predictive controller (NMPC). In the first one, a parametrized NMPC is used to approximate the action-value function of a regularized deep Expected Sarsa (RDES) algorithm, and serves as the current action-value function to compute the temporal difference error, while a neural network (NN) with a novel feature representation is adopted as the subsequent action-value function instead of a secondary NMPC. This new feature representation consists in adding the current NMPC parameter vector to the input training data of the NN. As a consequence, the NN is able to stabilize the learning performance. Additionally, using this NN allows to reduce the overall training time, without affecting the closed-loop performance.

The second method introduces a novel combination of NMPC-based gradient Expected Sarsa (GES) with convergence guarantees. This approach demonstrates that gradient temporal difference learning stabilizes the learning process and converges to an equilibrium point, even when nonlinearities are present in the NMPC function approximation.

Finally, we find that RDES method converges to the same optimal policy as GES method. However, the former achieves this outcome in half the training time compared to the latter,

while the latter provides convergence guarantees to a locally optimal solution or a stable equilibrium point.

Using NMPC as a function approximator for the optimal policy in reinforcement learning has opened new research pathways, especially in enhancing safety and applicability across diverse domains. NMPC-based policies inherently satisfy state and input constraints as well as safety requirements, thanks to their design. Furthermore, NMPC provides a degree of interpretability and insight in RL that is often absent in DNN-based approaches, as the parametrization weights in NMPC carry more meaningful significance.

#### REFERENCES

- [1] L. Grüne and J. Pannek, *Nonlinear Model Predictive Control*, 2nd ed. Cham, Switzerland: Springer, 2017.
- [2] T. P. Nascimento, C. E. T. Dórea, and L. M. G. Gonçalves, “Nonholonomic mobile robots’ trajectory tracking model predictive control: a survey,” *Robotica*, vol. 36, no. 5, pp. 676–696, 2018.
- [3] Z. Zhang, O. Babayomi, T. Dragicevic, R. Heydari, C. Garcia, J. Rodriguez *et al.*, “Advances and opportunities in the model predictive control of microgrids: Part i—primary layer,” *Int. J. Electr. Power Energy Syst.*, vol. 134, p. 107411, 2022.
- [4] R. S. Sutton and A. G. Barto, *Reinforcement Learning: An introduction*. MIT Press, 2018.
- [5] S. Gros and M. Zanon, “Data-driven economic NMPC using reinforcement learning,” *IEEE Trans. Autom. Control*, vol. 65, no. 2, pp. 636–648, 2019.
- [6] M. Zanon, S. Gros, and A. Bemporad, “Practical reinforcement learning of stabilizing economic MPC,” in *Proc. IEEE ECC*. IEEE, 2019, pp. 2258–2263.
- [7] A. B. Martinsen, A. M. Lekkas, and S. Gros, “Combining system identification with reinforcement learning-based MPC,” *IFAC-PapersOnLine*, vol. 53, no. 2, pp. 8130–8135, 2020.
- [8] A. B. Kordabad, H. N. Esfahani, A. M. Lekkas, and S. Gros, “Reinforcement learning based on scenario-tree MPC for ASVs,” in *Proc. ACC*. IEEE, 2021, pp. 1985–1990.
- [9] H. N. Esfahani, A. B. Kordabad, and S. Gros, “Approximate robust NMPC using reinforcement learning,” in *Proc. IEEE ECC*. IEEE, 2021, pp. 132–137.
- [10] H. Moradimaryamnegari, M. Frego, and A. Peer, “Model predictive control-based reinforcement learning using expected Sarsa,” *IEEE Access*, vol. 10, pp. 81 177–81 191, 2022.
- [11] A. B. Kordabad, D. Reinhardt, A. S. Anand, and S. Gros, “Reinforcement learning for mpc: Fundamentals and current challenges,” *IFAC-PapersOnLine*, vol. 56, no. 2, pp. 5773–5780, 2023.
- [12] H. MoradiMaryamnegari, M. Frego, and A. Peer, “Data-driven model predictive control using deep double expected Sarsa,” in *Proc. CODIT*. IEEE, 2023, pp. 345–350.
- [13] H. R. Maei, C. Szepesvári, S. Bhatnagar, and R. S. Sutton, “Toward off-policy learning control with function approximation,” in *ICML*, vol. 10, 2010, pp. 719–726.
- [14] H. Van Seijen, H. Van Hasselt, S. Whiteson, and M. Wiering, “A theoretical and empirical analysis of expected Sarsa,” in *Proc. IEEE ADPRL*. IEEE, 2009, pp. 177–184.
- [15] D. P. Kingma and J. Ba, “Adam: A method for stochastic optimization,” *arXiv preprint*, p. 1412.6980, 2014.
- [16] H. Maei, C. Szepesvari, S. Bhatnagar, D. Precup, D. Silver, and R. S. Sutton, “Convergent temporal-difference learning with arbitrary smooth function approximation,” *Advances in neural information processing systems*, vol. 22, 2009.
- [17] R. S. Sutton, H. R. Maei, D. Precup, S. Bhatnagar, D. Silver, C. Szepesvári, and E. Wiewiora, “Fast gradient-descent methods for temporal-difference learning with linear function approximation,” in *Proceedings of the 26th annual international conference on machine learning*, 2009, pp. 993–1000.
- [18] M. Sani, B. Robu, and A. Hably, “Dynamic obstacles avoidance using nonlinear model predictive control,” in *Proc. IECON*. IEEE, 2021, pp. 1924–1929.
- [19] J. A. E. Andersson, J. Gillis, G. Horn, J. B. Rawlings, and M. Diehl, “CasADi – A software framework for nonlinear optimization and optimal control,” *Math. Program. Comput.*, vol. 11, no. 1, pp. 1–36, 2019.